Contract No:

This document was prepared in conjunction with work accomplished under Contract No. DE-AC09-08SR22470 with the U.S. Department of Energy (DOE) Office of Environmental Management (EM).

Disclaimer:

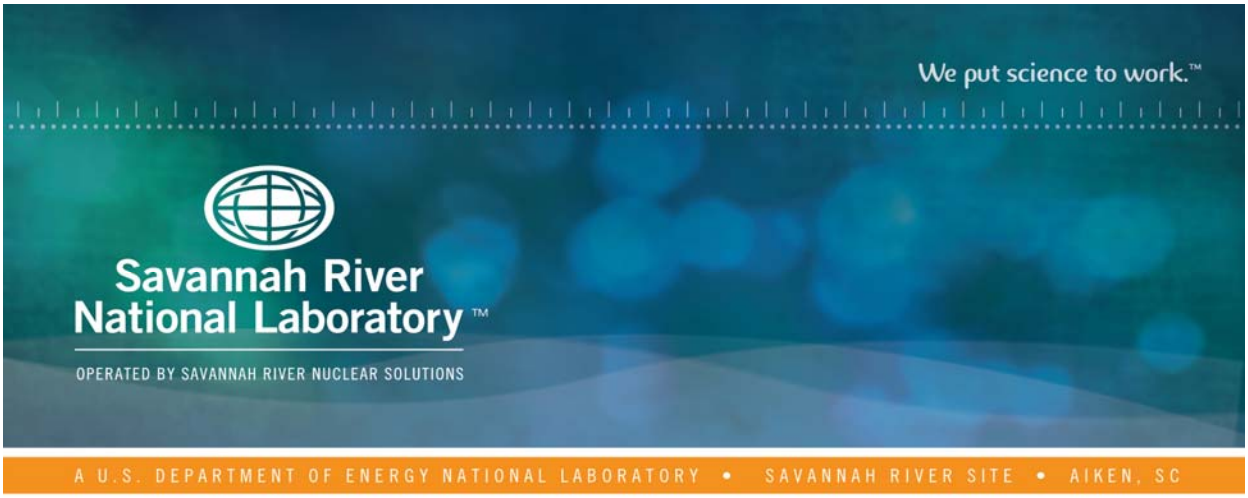

Preliminary Analysis of Species Partitioning in the DWPF Melter

A. S. Choi
M. R. Kesterson
F. C. Johnson
D. J. McCabe

July, 2015
SRNL-STI-2015-00279, Revision 0

DISCLAIMER

Printed in the United States of America

Prepared for
U.S. Department of Energy

SRNL-STI-2015-00279
Revision 0

Keywords: *DWPF Melter, Off-Gas Entrainment, Technetium, HTWOS Model*

Retention: *Permanent*

Preliminary Analysis of Species Partitioning in the DWPF Melter

A. S. Choi
M. R. Kesterson
F. C. Johnson
D. J. McCabe

July 2015

Prepared for the U.S. Department of Energy under contract number DE-AC09-08SR22470.

Savannah River National Laboratory™
OPERATED BY SAVANNAH RIVER NUCLEAR SOLUTIONS

REVIEWS AND APPROVALS

AUTHORS:

Alexander S. Choi, Process Technology Programs Date

Matthew R. Kesterson, Environmental Modeling Date

Fabienne C. Johnson, Engineering Process Development Date

Daniel J. McCabe, Hanford Mission Programs Date

TECHNICAL REVIEW:

F. G. Smith, Radiological Performance Assessment, Reviewed per E7 2.60 Date

APPROVAL:

E. N. Hoffman, Manager Date
Engineering Process Development, E&CPT Research Programs

C. C. Herman, Director Date
Hanford Mission Programs, Environmental Stewardship

A. P. Fellinger, Manager Date
Environmental & Chemical Process Technology (E&CPT) Research Programs

EXECUTIVE SUMMARY

The work described in this report is preliminary in nature since its goal was to demonstrate the feasibility of estimating the off-gas entrainment rates from the Defense Waste Processing Facility (DWPF) melter based on a simple mass balance using measured feed and glass pour stream compositions and time-averaged melter operating data over the duration of one canister-filling cycle. The only case considered in this study involved the SB6 pour stream sample taken while Canister #3472 was being filled over a 20-hour period on 12/20/2010, approximately three months after the bubblers were installed. The analytical results for that pour stream sample provided the necessary glass composition data for the mass balance calculations. To estimate the "matching" feed composition, which is not necessarily the same as that of the Melter Feed Tank (MFT) batch being fed at the time of pour stream sampling, a mixing model was developed involving three preceding MFT batches as well as the one being fed at that time based on the assumption of perfect mixing in the glass pool but with an induction period to account for the process delays involved in the calcination/fusion step in the cold cap and the melter turnover.

Some of the key findings of this study include:

- The proposed concept of estimating off-gas entrainment rates from measured feed and glass pour stream compositions appears feasible at least for the major species and thus additional case studies are warranted.

- The overall entrainment rate from the bubbled DWPF melter was calculated to be 2.4% of the calcined solids fed, which is ~2X the design basis entrainment rate for the non-bubbled melter.

- The average entrainment rate of the four major non-volatile sludge components, including Al, Fe, Mn and U, was calculated to be 2.7% fed, while that of the frit components, excluding Na, was 0.7%. It means that the entrainment rate of sludge is higher than that of frit by a ratio of 4:1, which is in qualitative agreement with the results of two off-gas deposit samples taken earlier.

- Specifically, the calculated entrainment rates of Fe and Si were 0.6-0.7%, while those of Al, B, Mn, Th and U were higher, ranging from 1.9 to 5.6% with Mn at the highest.

- The calculated entrainment rate of Na was 7.5%, of which a significant fraction could have been entrained via volatilization in the form of borates, sulfates, and halides.

- The calculated entrainment rates of semi-volatile Cs and Cd ranged from 16 to 18%, while that of sulfur was estimated to be higher than 50%.

- The calculated DWPF entrainment rates were in general higher than the DM1200 rates, which may be attributed in part to the formic acid used as the reductant for the DWPF feeds compared to sugar used for the DM1200 feeds, as demonstrated earlier in terms of increased pressure spikes with formic acid-based feeds. The much higher entrainment rates of Na and semi-volatiles in the DWPF melter could be reflective of actual operating conditions such as extended idling.

The proposed concept will be tested further against additional pour stream samples taken under different operating conditions (e.g., non-bubbled) and, if necessary, it will be adjusted and refined. In particular, work needs to be focused on resolving the flowrates and melter hold-up of various species in the process streams for an improved material balance. Work will also expand to include other isotopes besides Cs-137.

TABLE OF CONTENTS

LIST OF TABLES

LIST OF FIGURES

LIST OF ACRONYMNS

ARP	Actinide Removal Process
DCS	Distributed Control System
DF	Decontamination Factor
GPCP	Glass Product Control Program
HLW	High-Level Waste
HTWOS	Hanford Tank Waste Operations Simulator
LSFM	Large-Slurry Fed Melter
LAW	Low-Activity Waste
MCU	Modular CSSX Unit
MFT	Melter Feed Tank
SB	Sludge Batch
SBS	Submerged Bed Scrubber
SME	Slurry Mix Evaporator
SRAT	Sludge Receipt and Adjustment Tank
SRNL	Savannah River National Laboratory
SRS	Savannah River Site
VSL	Vitreous State Laboratory
WL	Waste loading
WTP	Waste Treatment Plant

1.0 Introduction

As part of the overall effort to support the technetium (Tc) management project at the Hanford site,[1] this task seeks to develop an improved capability for predicting the partitioning of species in the Low Activity Waste (LAW) melter system for integration into the Hanford Tank Waste Operations Simulator (HTWOS) flowsheet model.[2] Specifically, it is desired to know what fraction of some of the key radioactive and non-radioactive species fed would get entrained into the off-gas system and their subsequent fates in the condensate collection and treatment system. A staged approach to achieving this goal is outlined in the task plan;[2] (1) understanding of the HTWOS model construct, (2) data mining on off-gas carryover or entrainment preferentially from large-scale melters, (3) empirical modeling of melter entrainment, (4) first-principle modeling of vitrification process and aqueous electrolyte equilibria in the Submerged Bed Scrubber (SBS), and (5) integration of the species partitioning models into the HTWOS model.

In essence, the feed and glassy materials can enter the off-gas system in two ways. First, they can get airborne by a sudden surge of steam and calcine gases erupting from below. This is a physical mode of entrainment and is influenced by not only the melter design and operating variables such as the bubbling rate but the feed chemistry as well. The other mode of entrainment is chemical in nature; some species such as CsCl becomes volatile at the glass temperature of 1,150 °C and exits the melter as a vapor only to condense into aerosols when it becomes cooled downstream. Under normal feeding/pouring operation, particulate carryover is dominated by the physical entrainment. Under idling mode, however, particulate carryover decreases dramatically since it occurs by volatility only. Off-gas entrainment data is typically reported as the sum of both physical and vapor-pressure driven entrainments.

Stages 1 and 2 of the task plan listed above were completed in 2014. Particularly, the off-gas entrainment data collected during Stage 2 came from two sources; (1) DM1200 melter runs at the Vitreous State Laboratory (VSL) using both the high level waste (HLW) and LAW simulants for the Hanford Waste Treatment Plant (WTP) blended with glass-forming chemicals,[3] and (2) Large-Slurry Fed Melter (LSFM) runs at the Savannah River Site (SRS) using various DWPF feed simulants coupled with glass-forming frits.[4] (Note that only one reference is given here for each melter as an example instead of citing all the reports from which entrainment data was taken.) Both DM1200 and LSFM were targeted since they are relatively large in scale, each having a melt surface area equaling 42-45% of the DWPF melter. The methods of off-gas sampling and analysis used were similar; the off-gas was sampled isokinetically downstream of the film cooler and the particulate collected was characterized and quantified for the elemental mass balance. The entrainment rates were measured under different operating conditions by varying the bubbling rate and/or number of bubblers, feed chemistry, etc., and the data thus collected will form part of the basis for the empirical modeling in Stage 3.

In addition, an attempt was made in this study to find ways to utilize the DWPF melter data in estimating the species partitioning ratios in an actual radioactive production melter. The scope of data was limited to those already available since it is extremely difficult, if not impossible, to produce the necessary off-gas entrainment data in a radioactive environment while also avoiding interfering with the glass production operations and schedule. Unlike pilot melters, however, the DWPF melter has no capability to sample off-gas and, although samples of the off-gas deposit as well as the condensate have been taken and analyzed a few times since the radioactive startup in 1996, they are not adequate enough to yield any quantitative information necessary for the estimation of the species partitioning ratios. The data that can potentially yield such information is the composition of glass and its pour rate. Specifically, during each sludge batch (SB) campaign, the DWPF is required to take at least one glass sample to meet the objectives of the Glass Product Control Program (GPCP) and to complete the necessary Production Records so that the final glass product may be disposed of at a Federal Repository.[5] So the focus of this study was to determine

whether reasonable entrainment rates could be obtained by performing a mass balance between the feed and glass pour streams based on their measured compositions and rates. If successful, the results of all nine DWPF pour stream samples taken thus far could be added to the entrainment database consisting of the DM1200 and LSFM data.

2.0 Proposed Approach and Data Needs

Broadly speaking, the proposed approach is to calculate the melter entrainment rates simply as the difference between the feed and glass pour rates. One big constraint is the fact that the DWPF is required to sample and analyze only one pour stream sample per sludge batch (SB); on average, each SB has produced on the order of 500 canisters each containing 4,000 lb of glass. So it means that when the pour stream is sampled, all hardware and software components of the DWPF melter system must be in working order so that all crucial operating data is logged into the Distributed Control System (DCS) database flawlessly. Furthermore, it must be ensured that both the feed and pour stream samples are analyzed under strict adherence to the quality assurance (QA) procedures. The mass balance analysis is covered in detail in the next section and only the data required for the mass balance analysis is discussed in this section.

Figure 1 shows a simplified flow diagram of the processing units including the melter that provide necessary data. Tank 40 is a staging tank with over one-million gallon capacity where each washed sludge batch is stored. The composition of Tank 40 content is fully analyzed, including radioisotopes, as part of the sludge qualification process and its measured composition was used in this study as the reference point for estimating the concentrations of those species not measured downstream.

The Sludge Receipt and Adjustment Tank (SRAT) is where the sludge feed is brought in and neutralized with nitric acid and blended with input streams from the Modular CSSX Unit (MCU) and Actinide Removal Process (ARP). The pH of the SRAT content is further reduced by adding formic acid which also acts as a reducing agent for HgO and MnO_2 and boiled under a total reflux for an extended period of time to steam strip the Hg. The nitrite is also destroyed in the process. The resulting SRAT product is fully analyzed for elemental, anions, total U and Cs-137 but no other radioisotopes. The analytical results of SRAT product were used in this study primarily to confirm the results of charge-reconciliation done on the Slurry Mix Evaporator (SME) content.

The SRAT product is then transferred to the SME in a ~4.500 gallon batch and blended with frit. At the end of extended boiling, the remaining SME product is again fully analyzed for elemental, anions, total U and Cs-137 but no other radioisotopes. The SME product is then transferred to the Melter Feed Tank (MFT) in a ~4.500 gallon batch and gets diluted with H_2O every time the transfer pump is started and a constant trickle H_2O flow. The MFT content is neither sampled nor analyzed except that every 5^{th} MFT batch is analyzed for pH, density and total solids only. However, since no chemical reactions are taking place in the MFT, the compositions of the SME product and MFT content in principle should be the same on a dry basis, ignoring the effect of tank heel.

As a result, the analytical results of each SME batch were used in this study to develop the composition of the corresponding MFT batch. In order to account for the impact of melter hold-up on the glass pool and thus the pour stream compositions, it was necessary to develop four preceding SME batch compositions as well as that of the current batch in the calculation of the “matching” MFT batch composition for a given pour stream sample. Furthermore, when calculating the composition of each SME or MFT batch, the effect of the heel on the composition of the new batch was ignored in this study for the reasons given later in this report.

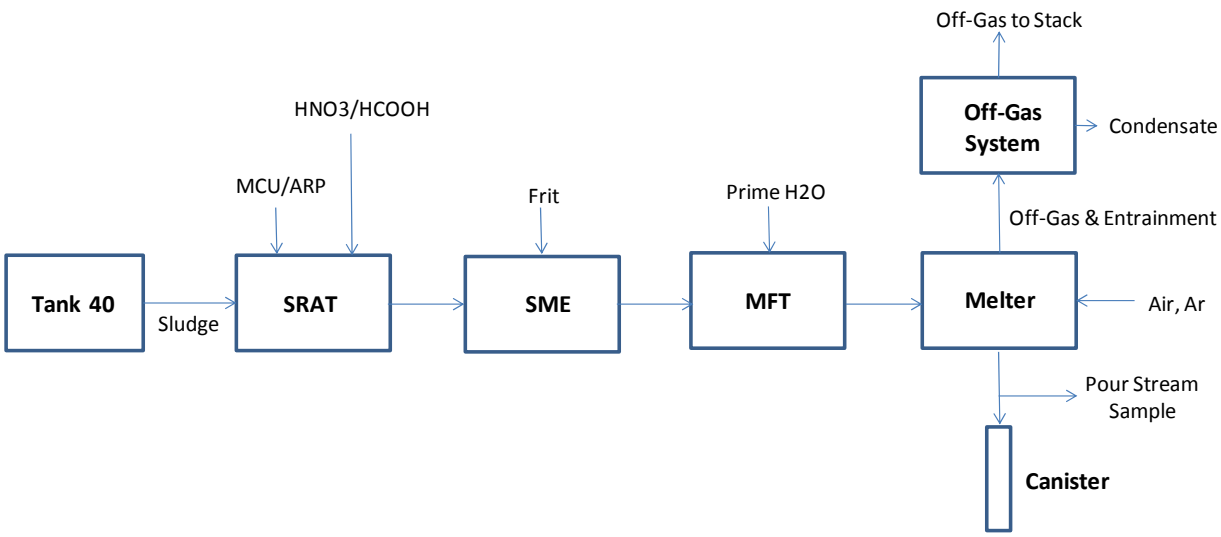

Figure 1. Schematic of DWPF Flowsheet.

3.0 Mass Balance Analysis

In actual melter operation, the composition of glass being poured is not necessarily the same as that of the calcined feed being fed at the same time because: (1) the feed composition can change appreciably from one Melter Feed Tank (MFT) batch to the next even when the sludge feed originates from the same Tank 40 batch, and (2) even under the perfect-mixing scenario, it would take several melter turnovers to flush out over 99% of a given batch of feed. One melter turnover is defined as when the cumulative volume of calcined feed equals one melt pool volume. At the nominal melt level of 32.7", the DWPF melter contains ~12,000 lbs of glass, which is enough to fill three canisters, and the nominal glass residence time is about 60 hours. Therefore, in order to calculate the off-gas entrainment rates of individual species as the balance between the feed and pour rates of a particular species *i*, it is essential to know the composition of the "composite" feed spanning several MFT batches that is representative of the melt pool composition at the time of pour stream sampling but without entrainment. For that, a mixing model is required that accounts for the effects of melt pool volume and residence time as well as the incoming feed composition on the pour stream composition.

3.1 Mixing Model

The "composite" feed composition was calculated by dividing the entire melter volume into three zones, the cold cap, melt pool and vapor space, and approximating each zone as a perfectly-mixed tank, as shown in Figure 2. In particular, noting that the non-volatile feed components decompose and undergo a series of calcination, redox and fusion reactions as they move downward in the cold cap, the progressive nature of the cold cap reactions has been modeled as a 4-stage countercurrent reactor with perfect-mixing in each stage at thermodynamic equilibrium.[6] It is noted that all the mass flows in Figure 2 represent time-averaged values over one canister-filling (pour) cycle under steady state feeding and pouring conditions.

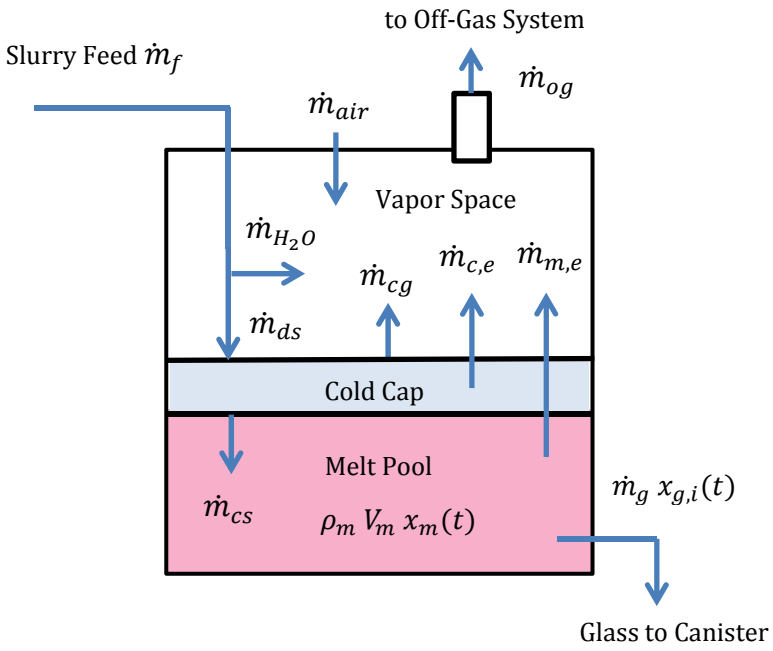

Figure 2. Schematic of Overall Mass Flows in Melter

The steady state mass balance for the entire melter is:

$$\dot{m}_f + \dot{m}_{air} = \dot{m}_g + \dot{m}_{og} \quad (1)$$

where $\dot{m}_f$ = slurry feed rate (lb/hr)
$\dot{m}_{air}$ = sum of air purge & inleakage rates (lb/hr)
$\dot{m}_g$ = glass pour rate (lb/hr)
$\dot{m}_{og}$ = off-gas flow rate (lb/hr)

The gas residence time in the DWPF melter vapor space is on the order of 5 seconds, during which calcine gases and volatile feed components undergo further reactions. However, the resulting changes in the molar concentrations of the off-gas are small since the flow rates of steam and air are dominating. As a result, the steady state overall mass balance suffices for the vapor space:

$$\dot{m}_{H_2O} + \dot{m}_{air} + \dot{m}_{cg} + \dot{m}_{c,e} + \dot{m}_{m,e} = \dot{m}_{og} \quad (2)$$

where $\dot{m}_{H_2O}$ = flow rate of water vapor from feed (lb/hr) = $\dot{m}_f\, x_{f,H_2O}$
$\dot{m}_{cg}$ = flow rate of calcine gases (lb/hr) = $\dot{m}_f\left(1 - x_{f,H_2O}\right)(1 - f_c)$
$\dot{m}_{c,e}$ = off-gas entrainment of cold cap species (lb/hr)
$\dot{m}_{m,e}$ = off-gas entrainment of melt species (lb/hr)
x_{f,H_2O} = mass fraction of water in slurry feed (lb/lb)
f_c = calcine factor (lb oxide/lb dried feed)

It is noted that the source of off-gas entrainment is split into two; carryover from the cold cap and the melt, which is qualitatively consistent with the results of off-gas deposit analysis;[7] the deposits were amorphous but contained such crystalline compounds as hematite (Fe_2O_3), nitratine ($NaNO_3$), magnetite (Fe_3O_4), and anhydrite ($CaSO_4$).

As for the cold cap, only the overall mass balance is considered in this preliminary study:

$$\dot{m}_{ds} = \dot{m}_{cs} + \dot{m}_{cg} + \dot{m}_{c,e} \quad (3)$$

where $\dot{m}_{ds}$ = dry feed rate (lb/hr) = $\dot{m}_f \left(1 - x_{f,H_2O}\right)$
$\dot{m}_{cs}$ = calcined feed rate (lb/hr) = $\dot{m}_f \left(1 - x_{f,H_2O}\right) f_c$

In a future study, the 4-stage cold cap model will be run in conjunction with a more comprehensive thermodynamic database in order to predict volatile melt species and further estimate their contributions to the overall off-gas entrainment.

Once the calcined solids (i.e., oxides) enter the melt pool, they spend the next 60 hours or so blending into the bulk melt and undergoing further redox and fining reactions before being discharged into a canister. In order to account for the impact of changing feed composition on the pour stream, the following unsteady state mass balance for species *i* is set up around the melt pool for a given pour cycle:

$$\rho_m V_m \frac{dx_{m,i}(t)}{dt} = \dot{m}_{cs}\, x_i(t) - \dot{m}_g\, x_{g,i}(t) - \dot{m}_{m,e}\, x_{me,i}(t) \quad (4)$$

where $x_{m,i}$ = mass fraction of species *i* in melt pool (lb/lb)
x_i = mass fraction of species *i* in calcined feed (lb/lb)
$x_{g,i}(t)$ = mass fraction of species *i* in pour stream
$x_{me,i}(t)$ = mass fraction of species *i* in melt entrainment (lb/lb)
ρ_m = melt pool density (lb/ft^3)
V_m = melt pool volume (ft^3)

As written, it is assumed in Eq. (4) that both the melt pool density (ρ_m) and volume (V_m) are constant. The validity of constant V_m was checked against the measured melt level data (whose DCS variable ID is LI3523) during a continuous feeding/pouring operation. For example, when Canister #3472 was being filled on 12/10/2010, the melt level remained at 32.7" with a relative standard deviation (RSD) of 0.2% throughout the 20-hr pouring operation. At the constant melt density (ρ_m) and volume (V_m),

$$\dot{m}_{cs} = \dot{m}_g + \dot{m}_{m,e} \quad (5)$$

Since the overall and individual species entrainment rates are unknown at this time, they are represented as a fraction of their respective pour rates:

$$\dot{m}_{m,e} = y\, \dot{m}_g \quad (6)$$

$$\dot{m}_{m,e}\, x_{me,i}(t) = y_i \dot{m}_g\, x_{g,i}(t) \quad (7)$$

where y and y_i are the fractions of the overall and individual species pour rates, respectively, that are entrained in the off-gas. Under the constant pour stream condition, the overall entrainment fraction y is related to the individual species entrainment fraction y_i as follows:

$$y = \sum_i y_i\, x_{g,i}(t) \quad (8)$$

Since $x_{g,i}(t) = x_{m,i}(t)$ under perfect-mixing conditions, Eq. (4) is re-written by substituting Eq. (5) to (7) for $\dot{m}_{cs}$ and $\dot{m}_{m,e}x_{me,i}(t)$ as:

$$\frac{dx_{g,i}(t)}{dt} = \frac{(1+y)\,\dot{m}_g}{\rho_m\,V_m}\,x_i(t) - \frac{(1+y_i)\,\dot{m}_g}{\rho_m\,V_m}\,x_{g,i}(t) \tag{9}$$

In principle, individual species entrainment fractions y_i can be estimated by iteratively solving Eq. (9) for $x_{g,i}(t)$ and y_i until the former matches the measured pour stream concentration of species *i*. The value of y_i thus determined should reflect the impact of not only the feed composition but the melter operating conditions such as the melt pool bubbling rate and the percentage of run time under feeding vs. idling conditions. However, such a solution over the entire duration of a given sludge batch (SB) campaign does not seem practically feasible considering the fact that since the radioactive startup in 1996 each SB campaign has produced on average over 500 canisters each containing nominally 4,000 lb of glass but with only one pour stream sample taken. So Eq. (9) was solved instead for each MFT batch up to the point where the pour stream sample was taken. The question is then: For how many previous MFT batches Eq. (9) needs to be solved repeatedly in order to determine the composition of the composite feed that is representative of a particular pour stream.

If all species are assumed to have the same entrainment ratio (i.e., $y = y_i$), Eq. (9) is further simplified as:

$$\frac{dx_{g,i}(t)}{dt} = \frac{(1+y)\,\dot{m}_g}{\rho_m\,V_m}\left(x_i(t) - x_{g,i}(t)\right) \tag{10}$$

For a given MFT batch, $x_i(t)$ is constant and Eq. (10) is integrated from $t = t_n$ to $t = t_{n+1}$ to get:

$$ln\left[\frac{x_i - x_{g,i}(t_{n+1})}{x_i - x_{g,i}(t_n)}\right] = -\left[\frac{(1+y)\dot{m}_g}{\rho_m V_m}\right](t_{n+1} - t_n) \tag{11}$$

It is noted that the term $\dot{m}_g/\rho_m V_m$ on the right side of Eq. (11) represents the reciprocal of time for one melter turnover in the absence of off-gas entrainment. Thus, if we define $N = (t_{n+1} - t_n)/\left(\rho_m V_m/\dot{m}_g\right)$, the right side of Eq. (11) without the negative sign represents the number of melter turnover in the presence of off-gas entrainment. In order to see the impact of entrainment on mixing, let's assume $x_i = 0$ and Eq. (11) is simplified to:

$$ln\left[\frac{x_{g,i}(t_{n+1})}{x_{g,i}(t_n)}\right] = -(1+y)\,N \tag{12}$$

As expected, the concentration of species *i* is shown in Figure 3 to decrease faster with increasing off-gas entrainment; it would take 4.6 melter turnovers to flush out 99% of species *i* initially in the tank at $y = 0$ and it decreases to 3.8 melter turnovers at $y = 0.2$. For the purpose of ensuring adequate tank mixing, it would be conservative to assume no entrainment since it requires more melter turnovers and thus more previous MFT batches to be considered in the mass balance. However, since the difference between 0% and 20% entrainment is less than one melter turnover, the impact of off-gas entrainment on tank mixing will not be large at the more representative entrainment ratios of less than 1 to 5 %.

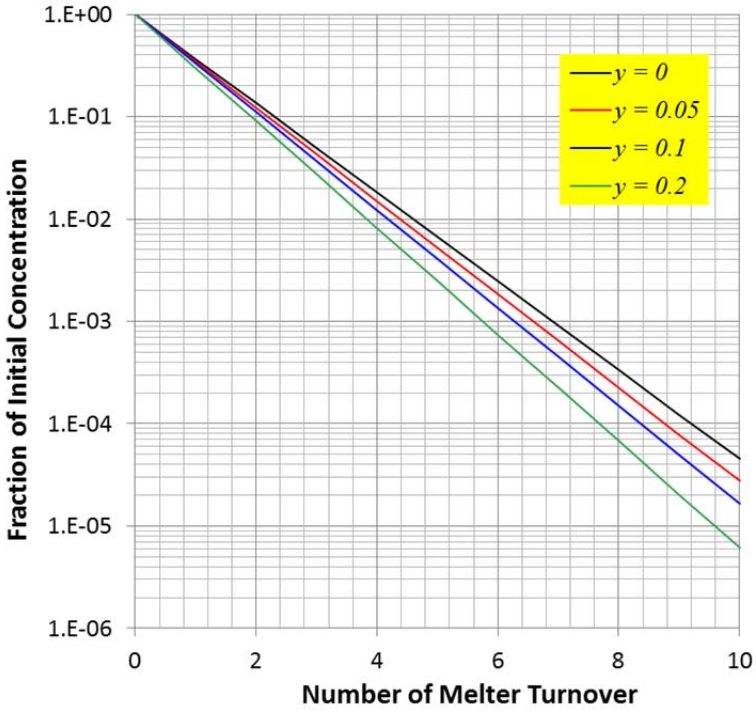

Figure 3. Tank Mixing vs. Number of Melter Turnover

Finally, rearrangement of Eq. (11) yields:

$$x_{g,i}(t_{n+1}) = x_i + \left[x_{g,i}(t_n) - x_i\right] \exp[-(1+y)N] \tag{13}$$

In this preliminary study, Eq. (13) was further simplified by assuming that y = 0, which allowed the individual species entrainment rates (y_i) to be estimated directly by comparing the calculated $x_{g,i}$ to the measured data without the need for iteration.

3.2 Case Study

As a test case for the methodology proposed in this task, the pour stream sample taken during the SB6 run was selected. The SB6 run began in June 2010 with the MFT batch 531 (MFT531) under non-bubbled conditions. The bubblers were installed in September 2010, and the SB6 pour stream sample was taken at 15:40 hour on 12/20/2010 while MFT551 was being fed at the argon bubbling rate of 5.2 scfm. Table 1 summarizes the operating history of four MFT batches, including MFT551 and three preceding batches MFT548-550. It is noted that MFT548-550 totaled ~13,000 gallons of feed, producing 12.5 canisters, which is equivalent to a little over 4 melter turnovers. According to Figure 3, >98% of the melt pool content remaining at the end of MFT547 would have been flushed out at the beginning of MFT551. Therefore, Eq. (13) may be applied with the composition of MFT548 as the initial melt pool composition. It is noted that the MFT551 data in Table 1 shows only the portion leading up to the pour stream sampling, which took place 74 hours after the start of MFT551. It is also noted that the total solids and thus the density of each MFT batch decreased with time since every time the feed pump is re-started, it needs to be primed with water along with a constant trickle of water into the MFT regardless of the melter or MFT operational status.

Table 1. Operating History and Feed Properties Leading up to SB6 Pour Stream Sampling.

Batch #	start feeding	stop feeding	total slurry fed (gal)	Avg. feed rate (gpm)	initial MFT density (g/ml)	ending MFT density (g/ml)	initial total solids (wt%)	ending total solids (wt%)	# of cans filled
548	11/25/2010 13:58	11/29/2010 4:06	4,595	0.889	1.31	1.268	37.4	33.34	4.53
549	11/29/2010 15:38	12/1/2010 23:29							
	12/8/2010 2:12	12/9/2010 23:59	4,382	0.719	1.308	1.237	37.62	30.58	4.48
550	12/10/2010 20:12	12/12/2010 18:19							
	12/13/2010 16:14	12/13/2010 17:22							
	12/13/2010 21:53	12/15/2010 16:22	3,994	0.742	1.282	1.243	38.9	33.72	3.44
551	12/17/2010 13:17	12/20/2010 15:40	4,359	0.958	-	1.220	-	39.70	3.01

3.2.1 Mass Balance Equations

Eq. (13) was applied for each successive MFT batch using MFT548 as the starting melt pool composition as follows:

$$MFT549: \quad x_{g,i}(549) = x_i(549) + \left[x_{g,i}(548) - x_i(549)\right] \exp[-N_{549}] \tag{14}$$

$$MFT550: \quad x_{g,i}(550) = x_i(550) + \left[x_{g,i}(549) - x_i(550)\right] \exp[-N_{550}] \tag{15}$$

$$MFT551: \quad x_{g,i}(551) = x_i(551) + \left[x_{g,i}(550) - x_i(551)\right] \exp[-N_{551}] \tag{16}$$

where $x_i(n)$ represents the composition of the n^{th} MFT batch on a calcined solids basis and $x_{g,i}(n)$ the melt pool composition at the end of the n^{th} MFT batch feeding. The exception is that both N_{551} and $x_{g,i}(551)$ are evaluated at the time of pour stream sampling rather than at the end of MFT551 feeding.

Finally, the rate of off-gas entrainment for species *i* was calculated as follows:

$$\dot{m}_{e,i} = \dot{m}_{cs}(551)\, x_{g,i}(551) - \dot{m}_g(3472)\, x_{ps,i}(3472) \tag{17}$$

where $\dot{m}_{cs}(551)$ and $\dot{m}_g(3472)$ are the time-averaged calcine solids feed and pour rates, respectively, over the duration of Canister #3472 filling cycle and $x_{ps,i}(3472)$ is the measured concentration of species *i* in the pour stream that filled Canister #3472. With the exclusion of the cold cap modeling in this study, Eq. (17) was applied on an elemental basis rather than on an oxide basis.

3.2.2 MFT Batch Chemistry

Available analytical data for the Slurry Mix Evaporator (SME) products are shown in Table 2. Instead of using the measured data as given, any charge imbalance that existed in the data was reconciled first under the constraints of measured bulk properties such as pH, density and total and calcined solids. In doing so, the measured Na concentrations were adjusted by -2 to 11%, which indicates that the SME data used were in line with the expected analytical uncertainty of ±10%. It is noted that 80% of measured Ca and 60% of measured Mn were assumed to be soluble. Since the concentration of carbonate ion was not measured, it was calculated to be the difference between the equivalent molar cation and anion concentrations. The resulting concentrations of total inorganic carbon (TIC) were found to be in line with the measured data for the corresponding SRAT products.

The charge-reconciled elemental and ionic data were next converted into the SME product compositions on a neutral-species basis, as shown in Table 3 for SME548 as an example. These compositions are used as the input for the cold cap model to predict the composition of calcine gases (i.e., $\dot{m}_{cg}$ and $\dot{x}_{cg,i}$) as well as the volatile melt species at 1,150°C (i.e., volatile portion of $\dot{m}_{c,e}$). As stated previously, however, the cold cap model run was excluded from this preliminary study, and the cold cap entrainment term ($\dot{m}_{c,e}$) was lumped into that of the melt ($\dot{m}_{m,e}$). As a result, the mass balance analysis can only be performed in terms of calcined solids or the elements that make up the glass oxides, while those elements that make up the calcine gases and volatiles/semi-volatiles such as C, N, H and halides were excluded.

Once the SME product is transferred to the MFT, it is blended with the heel and diluted. Since the MFT content is no longer sampled and analyzed for the full elemental and ionic distributions, the elemental composition of each MFT batch was calculated simply by multiplying the elemental composition of the corresponding SME batch by the dilution factor to account for the addition of pump prime H_2O as well as trickled H_2O flow. However, since every 5th MFT batch is still analyzed only for the bulk properties, the total solids contents of some MFT batches thus calculated were compared to the measured values and the agreement between the calculated and measured values has been good, typically within ±5%.

The calculated elemental compositions of MFT548 to 551 are compared in Table 4 to that of Tank 40; note that these compositions represent $x_i(n)$ in Eqs. (14) - (16). As expected, the sludge components such as Al, Fe, Na and Mn show a significant decrease in concentration from Tank 40 because of; (1) dilution by the frit addition and (2) the difference in composition bases used - the composition of Tank 40 is on a total solids (TS) basis, while the MFT batches are on a slurry basis. The frit components such as B, Li and Si all show an expected increase over their respective Tank 40 values and so does Ti due to the input from the Actinides Removal Process (ARP) to MFT550/551. The Cs-137 concentration remains approximately the same, which is a reflection of the input from the Modular CSSX Unit (MCU).

Compared to the Tank 40 results shown in Table 4, the SME product analysis was rather limited in scope; most of the minor species including the noble metals were not measured, and Cs-137 was the only isotope measured. As a result, those MFT concentrations in blue and asterisked were estimated by iteration until their calculated ratios to Fe (e.g., Ba/Fe) matched their respective ratios in Tank 40. This is a reasonable approximation, except for Sr, since they are neither added/removed nor expected to undergo chemical changes during the SRAT/SME processing. The concentrations of Be, Sb, Sn, Tc-99 and V are excluded from Table 4 because they are reported as below the detection limits in both Tank 40 and pour stream sample results.

Table 2. Comparison of SB6 SME Product Analytical Data.

SME Batch #	548	549	550	551
Elements	(wt% calcine)	(wt% calcine)	(wt% calcine)	(wt% calcine)
Al	5.112	5.417	4.305	5.007
B	1.377	1.460	1.511	1.446
Ca	0.407	0.458	0.348	0.413
Cr*	0.024	0.027	0.033	0.024
Cu*	0.035	0.027	0.017	0.026
Fe	6.781	6.915	5.505	6.307
K	0.039	0.491	0.145	0.075
Li	2.097	2.310	2.345	2.230
Mg	0.221	0.236	0.180	0.211
Mn	1.997	2.035	1.620	1.913
Na*	10.791	9.974	10.900	11.144
Ni	0.899	0.884	0.678	0.809
Si	21.207	22.609	22.723	22.170
Ri	0.010	0.028	0.364	0.218
U*	1.795	1.759	1.422	1.779
Zr*	0.13	0.14	0.11	0.13
Total	52.917	54.766	52.209	53.907
Anions	(mg/kg)	(mg/kg)	(mg/kg)	(mg/kg)
NO_3	24,273	19,806	24,875	21,827
COOH	34,579	36,626	44,274	38,509
C_2O_4	<493	< 501	796	< 538
SO_4	1,200	1,094	1,341	1,251
NO_2	<493	< 501	< 548	< 538
F	<493	< 501	< 548	< 538
Cl	<493	< 501	< 548	< 538
PO_4	<493	< 501	< 548	< 538
calc'd CO_3 for charge balance	4,169	5,637	3,455	5,243
Misc.				
TOC (mg/kg)	13,390	14,070	15,207	14,934
Hg (mg/kg)	1,025	1,016	163	771
Cs-137 (Bq/g)	33,760,000	50,766,667	59,407,146	62,670,000
Bulk Properties				
Density (g/ml)	1.348	1.333	1.314	1.365
Total Solids (wt%)	39.87	40.12	43.67	43.69
Calcined Solids (wt%)	33.43	33.78	37.16	37.22
pH	10.4	10.1	9.4	9.4

* ICP by mixed acid; otherwise, by peroxide fusion

Table 3. Charge-Reconciled Composition of SME548.

Insoluble Solids	g/L slurry		Soluble Solids	g/L slurry
Fe(OH)3	60.7173		Ca(COOH)2	0.8194
Al(OH)3	69.1460		Ca(NO3)2	0.5267
MnO2	8.870		CsCOOH	0.0087
Ca(OH)2	2.8177		CsNO3	0.0049
Na2U2O7	11.1850		KCOOH	0.2612
Mg(OH)2	2.4775		KNO3	0.1600
HgO	1.4922		Mn(COOH)2	6.5322
Ni(OH)2	6.6455		Mn(NO3)2	4.1094
Cr(OH)3	0.1900		NaCl	0.5478
Cu(OH)2	0.2323		NaF	0.1469
TiO2	0.0755		NaCOOH	63.2279
SiO2	212.2845		NaNO3	40.2735
Na2O	21.7744		NaNO2	0
ThO2	0		Na3PO4	0.2295
Zn(OH)2	0		Na2CO3	5.2296
PuO2	0		Na2C2O4	1.0119
RuO2	0		Na2SO4	2.3912
RhO2	0		Total Soluble	125.4808
PdO	0		calc'd H2O	782
Cd(OH)2	0			
Sr(OH)2	0		Total Solids (TS)	577.1460
B2O3	20.7383		Measured TS	537.5922
Li2O	21.1171		Δ	7.36%
ZrO2	0.8027		Δ (exc. antifoam)	5.29%
BaSO4	0			
Sn(OH)2	0			
PbSO4	0			
TcO2	0			
La(OH)3	0			
antifoam	11.0991			
Total Insoluble	451.6653			

Table 4. Comparison of MFT Batch Compositions to Tank 40.

Element	Tank 40	MFT548	MFT549	MFT550	MFT551
	(wt% TS)	(wt% slurry)	(wt% slurry)	(wt% slurry)	(wt% slurry)
Al	10.6	1.5159	1.5549	1.3301	1.6933
B	< 0.009	0.4082	0.4190	0.4669	0.4889
Ba*	0.093	0.0133	0.0131	0.0113	0.0141
Be	< 0.00087				
Ca	0.868	0.1207	0.1315	0.1074	0.1398
Cd*	0.0314	0.0044	0.0043	0.0038	0.0047
Ce*	0.147	0.0211	0.0208	0.0179	0.0224
Co*	0.00869	0.0012	0.0011	0.0010	0.0013
Cr	0.0419	0.0061	0.0062	0.0080	0.0068
Cs-137	4.45E-04	3.12E-04	4.54E-04	5.72E-04	6.60E-04
Cu	0.0598	0.0096	0.0078	0.0056	0.0091
Fe	14	2.0110	1.9850	1.7007	2.1329
Gd*	0.0825	0.0119	0.0118	0.0100	0.0126
Hg	3.17	0.0909	0.0864	0.0136	0.0701
K	< 0.064	0.0116	0.1409	0.0245	0.0254
La*	0.0742	0.0107	0.0105	0.0090	0.0113
Li	0.0237	0.6218	0.6632	0.7246	0.7542
Mg	0.447	0.0654	0.0652	0.0557	0.0714
Mn	4.3	0.5921	0.5841	0.5006	0.6470
Mo*	0.00579	0.0007	0.0009	0.0007	0.0009
Na	13.2	3.3601	3.1781	3.7381	3.6934
Ni	1.83	0.2667	0.2538	0.2142	0.2735
Nd*	0.0262	0.0039	0.0037	0.0033	0.0040
P*	0.0764	0.0110	0.0109	0.0093	0.0117
Pb*	0.0242	0.0034	0.0034	0.0029	0.0036
Pd*	0.003	0.0004	0.0004	0.0004	0.0005
Pu*	0.01	0.0014	0.0014	0.0012	0.0015
Rh*	0.02	0.0029	0.0028	0.0024	0.0030
Ru*	0.09	0.0129	0.0128	0.0109	0.0137
S	0.23	0.0342	0.0314	0.0363	0.0370
Si	0.844	6.2892	6.4902	7.0208	7.4975
Sr*	0.0449	0.0065	0.0063	0.0054	0.0068
Th*	2.23	0.3203	0.3162	0.2710	0.3398
Ti	0.0189	0.0029	0.0081	0.1125	0.0738
U	3.68	0.5323	0.5050	0.4392	0.6015
Zn*	0.0432	0.0062	0.0062	0.0053	0.0066
Zr	0.0822	0.0377	0.0390	0.0353	0.0452
Total	56.4064	16.4089	16.5767	16.9003	18.7200

** MFT concentrations are estimates from Tank 40 data by matching their ratios to Fe (also shown as blue text)*

3.2.3 Bases and Assumptions

Some of the key bases and assumptions discussed thus far are re-summarized as follows:

1. Available analytical results for the SB6 pour stream sample taken at 15:40 hour on 12/20/2010 provided the necessary glass composition for the mass balance.[5]
2. The melter operating data, including the feed and pour rates, i.e., $\dot{m}_{cs}(551)$ and $\dot{m}_{g}(3472)$ in Eq. (17), respectively, were time-averaged over the duration of Canister #3472 filling cycle.[8]
3. The number of preceding MFT batches to be included in the calculation of the "composite" feed composition was set at the value which would result in a sufficient number of melter turnovers to flush out 99% of the old melt pool composition under perfect mixing without off-gas entrainment.
4. MFT548 represents the initial melt pool composition for the calculation of the composite feed composition that can be coupled to the pour stream composition of Can #3472, i.e., $x_i(548) = x_{g,i}(548)$ in Eq. (14).
5. The melt pool is a perfectly-mixed tank with an induction period of one melter turnover (or glass residence time) plus the calcination time.
6. The effect of heel in the MFT batch mixing is ignored.

Table 5 lists the values of the key operating parameters used to calculate the entrainment rates. It is noted that the number of melter turnovers achieved during the MFT551 feeding (N_{551}) up to the point where the pour stream sample was taken is given as 0.25, whereas the number of canisters produced during the same period is given as 3.01 in Table 1, which is essentially equivalent to one melter turnover. These seemingly contradictory results came about as a result of Assumption #5. Specifically, the use of induction period in Assumption #5 is an attempt to inject realism into the perfect-mixing assumption. Even though the cold cap portion of the entrainment analysis has been excluded in this study, the reality is that it would take a significant amount of time before a new species being fed as part of the slurry feed shows up in the pour stream on the other end. It can be further inferred from Table 1 that by the time the pour stream sample was taken, MFT551 had been feed for over 74 hours. However, when the assumed 2-hour calcination time and 57.5 hours of glass residence time are subtracted, the actual duration of MFT551 feeding that impacted the pour stream composition is reduced to ~15 hours or 0.25 melter turnover at the given calcine feed rate of 216.5 lb/hr.

The calcination time is the time required for the slurry feed to completely convert to oxides in the cold cap, during which it undergoes the dehydration, decomposition/calcination and fusion reactions. The basis for the assumed 2-hr calcination time is the data from a recent 1/12th scale melter run,[9] which showed that the evolution of H_2/CO (from the formate decomposition) stopped 10 minutes after the feeding stopped but NO/NO_2 continued to evolve even after 1 hour at more than 1/3 of the nominal rate during feeding. It was also observed during the LSFM 5th Run that it took 2 to 3 hours to complete cold cap burn-off to a clear melt surface.[10]

Assumption #6 significantly reduces the time and effort involved in the mining, (if necessary) adjustment, and manipulation of the melter operating as well as the MFT batch chemistry and property data. However, as more MFT batches are included in the "composite" feed calculation, the impact of excluding the heels should decrease, which will be confirmed in a future study by including the effect of heel in the MFT batch mixing model.

Table 5. Operating Parameters Used in Entrainment Calculation.

Parameters	Value
Melter turnover:	
- N_{548}	1.17
- N_{549}	1.12
- N_{550}	1.09
- N_{551}	0.25
Mass flow rate:	
- $\dot{m}_{cs}(551)$ (lb/hr)	216.5
- $\dot{m}_{g}(3472)$ (lb/hr)	211.4
Can #3472 filling cycle (hr)	19.9
MFT551:	
- density (g/ml)	1.22
- total solids (wt%)	36.27
- calcination time (hr)	2
- glass residence time (hr)	57.5

3.2.4 Calculation Steps

The derivation of several mass balance equations have been discussed above in detail. A summary of the calculation steps that were followed in this study is given next:

1. Available analytical data for SME548-551 in Table 2 were charge reconciled by using Na as the adjustable parameter.
2. Calculate dilution factors from measured SME/MFT properties.
3. Calculate the compositions of MFT548-551 in Table 4 by reducing the charge-reconciled SME548-551 compositions by their respective dilution factors.
4. Calculate the number of melter turnovers ($N_{548} - N_{551}$) using the data given in Table 1. Reduce N_{551} per Assumption #5.
5. Calculate $x_{g,i}(551)$ by solving Eq. (14) to (16) in succession.
6. Calculate the off-gas entrainment rate of species *i* using Eq. (17) along with the mass flow data for MFT551 and pour stream given in Table 5.

4.0 Results and Discussion

4.1 Overall Entrainment Rate

Using Eq. (5) and the associated mass flow data in Table 5, the overall rate of entrainment is calculated to be 5.1 lb/hr or 2.4% of the calcined feed at the time Canister #3472 was being filled under bubbled conditions. It is noted that this rate is more than 2X the original design basis glass entrainment rate of 1% for the non-bubbled DWPF melter,[11] which was expected since melter pressure spikes are larger and more frequent under bubbled conditions, as shown in Figure 4,[12] and it is the large melter pressure spikes that induce large off-gas surges by which the feed/glassy materials are lifted up and entrained in the melter exhaust. In a future study, the pressure spike data will be examined more closely, including those taken during non-bubbled operation, to determine if there is a correlation between the frequency and magnitude of off-gas surges and the rate of off-gas entrainment.

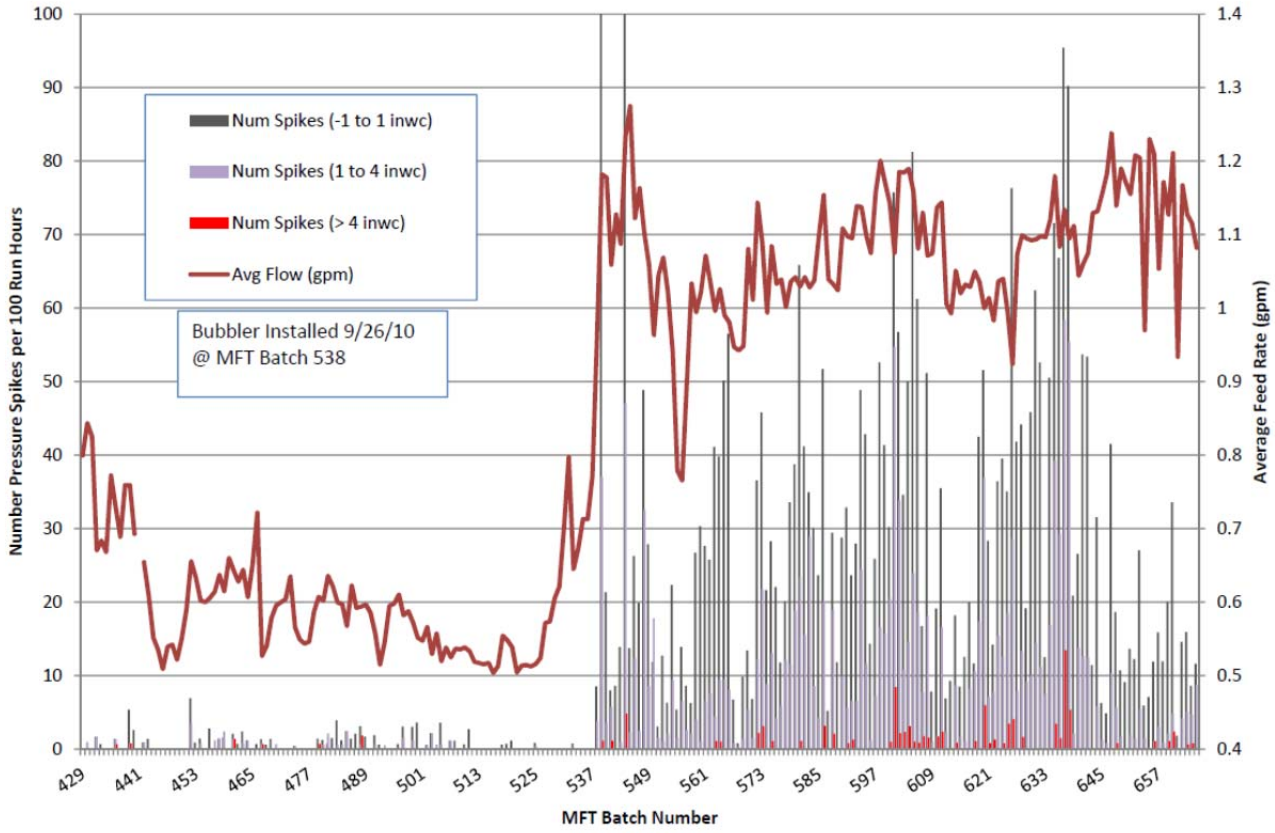

Figure 4. DWPF Melter Pressure Spike Before and After Bubbler Installation [Ref. 12].

4.2 Elemental Entrainment Rates

The results of the elemental mass balance calculations via Eq. (17) are summarized in Table 6 along with the resulting elemental entrainment rates. Also shown are the calculated composition of the "composite" MFT batch and the measured SB6 pour stream composition. It should be noted that the reported SB6 pour stream composition was obtained by averaging the eight replicates, four each from aqua regia (AR) and sodium peroxide fusion (PF) sample dissolution preparations except for Ca, K, Na, S and Zr by AR only and Si by PF only.[5] On the other hand, the pour stream composition shown in Table 6 is based only on the AR results except for Si with the aim of maintaining analytical consistency; more importantly, it resulted in entrainment rates that seem less conservative.

The average entrainment ratio of the four major sludge components with concentrations > 1 wt% (Al, Fe, Mn and U) was 2.7% of what was fed (or 2.7% fed in short), while that of the frit components (B, Li and Si) was lower at 0.7% fed. Furthermore, the instantaneous entrainment rate of the four major sludge components combined was 0.82 lb/hr, which is 2X that of the three frit components combined. These results are in a qualitative agreement with the earlier findings. For example, the off-gas deposit sample taken at the inlet of the Quencher during non-bubbled operation in early 2007 was determined to consist of approximately 90% sludge and 10% frit components.[7,13] If it is assumed that the 90:10 ratio represented the actual entrainment behavior of the non-bubbled melter, the results of this study suggest that use of the glass bubblers would make the frit more prone to entrainment. The quencher deposit sample was analyzed again in 2011 (soon after the data used in this study was collected) and it was found to be compositionally similar to mercury-enriched but frit-deficient SB6 melter feed.[14] Unfortunately, neither studies were able to determine the quantitative entrainment rates in terms of % fed.

Table 6. Elemental Mass Flows of Composite Feed, Pour Stream and Off-Gas Entrainment.

Element	Tank 40	Composite MFT		SB6 Pour Stream		Off-Gas Entrainment	
	(wt% TS)	(wt% slurry)	(lb/hr)	(wt%)	(lb/hr)	(lb/hr)	(% fed)
Al	10.6	1.4651	10.2654	4.6975	9.9294	0.3360	3.3
B	< 0.009	0.4582	3.2104	1.4900	3.1495	0.0609	1.9
Ba*	0.093	0.0124	0.0868	0.0524	0.1107	-0.0239	-27.6
Ca	0.868	0.1199	0.8399	0.4350	0.9195	-0.0796	-9.5
Cd*	0.0314	0.0041	0.0290	0.0112	0.0237	0.0053	18.2
Ce*	0.147	0.0197	0.1379	0.0650	0.1374	0.0004	0.3
Cr	0.0419	0.0072	0.0507	0.1103	0.2330	-0.1824	-359.8
Cs-137	4.45E-04	0.0005	0.0038	0.0015	0.0032	0.0006	16.4
Cu	0.0598	0.0071	0.0496	0.1708	0.3609	-0.3114	-628.2
Fe	14	1.8720	13.1166	6.1600	13.0208	0.0958	0.7
Gd*	0.0825	0.0111	0.0775	0.0396	0.0838	-0.0063	-8.1
Hg	3.17	0.0454	0.3181	0.0000	0.0000	0.3181	100
K	< 0.064	0.0442	0.3097	0.0788	0.1666	0.1431	46.2
La*	0.0742	0.0099	0.0693	0.0359	0.0758	-0.0065	9.3
Li	0.0237	0.7114	4.9846	2.3375	4.9409	0.0437	0.9
Mg	0.447	0.0616	0.4319	0.2040	0.4312	0.0007	0.2
Mn	4.3	0.5552	3.8902	1.7375	3.6727	0.2175	5.6
Mo*	0.00579	0.0008	0.0055	0.0042	0.0089	-0.0034	-61.0
Na	13.2	3.5969	25.2022	11.0250	23.3043	1.8979	7.5
Ni	1.83	0.2387	1.6722	0.8355	1.7661	-0.0938	-5.6
P*	0.0764	0.0102	0.0718	0.0724	0.1531	-0.0813	-113.3
Pb*	0.0242	0.0032	0.0224	0.0145	0.0307	-0.0083	-36.9
Pd*	0.003	0.0004	0.0028	0.0020	0.0042	-0.0014	-50.4
Ag*	0.01	0.0013	0.0094	0.0080	0.0169	-0.0075	-80.5
Rh*	0.02	0.0027	0.0187	0.0100	0.0211	-0.0024	-12.8
Ru*	0.09	0.0120	0.0843	0.0500	0.1057	-0.0214	-25.4
S	0.23	0.0354	0.2482	<0.0597	< 0.1261	> 0.1220	> 49.2
Si	0.844	6.9684	48.8256	22.9500	48.5110	0.3145	0.6
Sr*	0.0449	0.0060	0.0419	0.0214	0.0452	-0.0034	-8.1
Th*	2.23	0.2982	2.0896	0.9473	2.0023	0.0873	4.2
Ti	0.0189	0.0762	0.5337	0.2148	0.4539	0.0798	15.0
U	3.68	0.4943	3.4632	1.5600	3.2975	0.1657	4.8
Zn*	0.0432	0.0058	0.0406	0.0500	0.1057	-0.0651	-160.4
Zr	0.0822	0.0383	0.2686	0.0874	0.1847	0.0839	31.2
Total	56.5571	17.1985	120.5049	55.5917	117.5080	2.9640	-

** MFT concentrations are estimates (from Tank 40 data); they were used to estimate entrainment ratios (also shown as blue text). Negative values for entrainment (shown in red) indicate that the method of matching the ratios to Fe cannot yield meaningful results for these minor components likely because of their high sensitivity to variations in input data.*

The two most dominant sludge components, Al and Fe, were expected to exhibit similar entrainment rates. However, under bubbled conditions, 0.7% of Fe fed was entrained, while for Al it was nearly 5X higher at 3.3%. Furthermore, the instantaneous entrainment rate of Al was 3.5X higher than that of Fe despite the fact that its concentration was lower than Fe by more than 20%. While the calculated entrainment rate of Fe seems reasonable under bubbled conditions, that of Al is considerably higher than expected. It may be postulated that aluminum leached out of the K3 refractory (which contains alumina nominally at 60 wt%) considering the fact that the current DWPF Melter #2 has been in operation for over 13 years, including the last 4 years under bubbled conditions. However, this scenario would increase not only the entrainment but pour rates as well, which could lead to a negative entrainment ratio.

This leaching from melter components appears to be the case for Cr whose entrainment ratio was -360% fed. First, its concentration in the feed was lower than either Al or Fe by more than two orders of magnitude so even a slight change in the MFT analytical data or metal leaching/corrosion rates could have had a very large impact on its calculated entrainment rate. Second, chromium is a major constituent of both K-3 refractory (27 wt% as Cr_2O_3) and Inconel 690™ (27-31 wt%) electrodes. Thus, considering that the current DWPF melter has been in continuous operation for over 13 years, additional Cr could have entered the glass pool from the leaching of either K-3 or Inconel 690™, more likely the latter unless chromium could selectively leach out of K-3. Nickel also showed a negative entrainment ratio of -5.6% fed. However, since its concentration in the feed was more than 30X higher than that of Cr, its calculated entrainment ratio should have been less sensitive to the variations in analytical data or leaching/corrosion rates. Thus, the fact that ~60 wt% of Inconel 690™ is made up of Ni suggests that the negative entrainment rate of Ni may have been due to leaching of Inconel 690™. This scenario is likely if the electrodes are in or near the path of rising Ar bubbles, as demonstrated in a recent melter study using a coupon inserted into the melt pool directly in the path of Ar bubbles.[15] It will be interesting to see whether the entrainment rate of Ni still remains negative when the calculations are repeated in a future study using the data taken during non-bubbled operation.

All the minor components in blue text and asterisked, whose MFT concentrations were estimated by matching their ratios to Fe to their respective ratios in Tank 40, showed negative entrainment rates except for Th. This suggests that the method of matching the ratios to Fe cannot yield meaningful results for these minor components likely because of their high sensitivity to variations in input data, as discussed above. This postulation is supported by the fact that although estimated also by matching the ratios to Fe, the resulting concentration of Th in the MFT batch was on par with such sludge components as Mn and Ni, and its calculated entrainment ratio was positive at 4.2% fed. However, it is not clear why the results for all the minor components were uni-directional (i.e., all negative entrainment) instead of random. The exception is Sr, whose negative entrainment rate was likely due to the fact that the additional input of Sr into the SRAT from the ARP transfer was not accounted for.

Sodium was the second most abundant species in the feed after Si and, except for the semi-volatiles such as Cd and Cs, it showed the highest entrainment ratio of 7.5% fed. However, sodium was excluded from either the sludge or frit entrainment ratio calculations because 68% and 32% of the total Na came with the sludge and frit, respectively, according to the results of charge reconciliation. If the average entrainment ratios of sludge and frit calculated above (i.e., 2.7 and 0.7%, respectively) were to be combined at a ratio of 68:32, the total entrainment ratio of Na would be 2.1% fed, which is considerably lower than 7.5%. This suggests that a significant portion of the entrained Na was likely due to volatilization by forming the alkali-rich borates, sulfates and halides.[16]

Of the three remaining frit components, boron had the highest entrainment ratio of 1.9% fed, which is approximately 2X and 3X higher than those of Li and Si, respectively. And this was expected since the volatility of boron at the melt temperature of 1,150 °C has previously been observed.[17] The calculated entrainment ratio of Si was 0.6% fed, which is within the expected range for the non-volatile species, while that of Li was higher at 0.9% fed, which may be attributed to the formation of volatile alkali salts.

As expected from their relative volatilities, the calculated entrainment ratios of Cd and Cs-137 were high at 18.2 and 16.4% fed, respectively. Although these values are considerably higher than the other feed components, they still seem reasonable considering that the original design basis entrainment ratio of Cs is 10% under non-bubbled conditions.[11] Since the measured concentration of sulfur in the pour stream was below detection limit, only the lower bound of its entrainment ratio was calculated to be 49% fed.

4.3 Comparison to Other Melter Data

In order to find out how the calculated entrainment rates in this study compare to other melter data, one of the melter emission studies performed at the Vitreous State Laboratory (VSL) was used as the basis for comparison. In particular, the data taken from their largest pilot melter DM1200 was used since off-gas entrainment is strongly scale-dependent with all other conditions being equal. In one such run,[3] the HLW AZ-101 simulants were fed along with the glass-forming chemicals (in lieu of frit) under different bubbler configurations. In Table 7, the calculated elemental entrainment ratios in this study are compared to those measured at two different bubbling rates in DM1200.

A clear trend in the bubbling rate vs. entrainment is shown in the DM1200 data; when the bubbling rate was doubled, the measured entrainment rates were also doubled more or less for all species. The general trend of increasing entrainment with increasing bubbling rate or, more accurately, increasing bubbling flux (defined as the volumetric bubbling rate per unit melt surface area) was expected since particulates would get airborne more easily at a higher linear velocity of bubbling medium. The support for this postulation comes from the same DM1200 data;[3] when the number of bubblers was doubled to four at the same total bubbling rate thereby reducing the linear bubbling velocity by half, the measured entrainment rates decreased for all species as a result.

A direct comparison between the DWPF and DM1200 entrainment rates is not straightforward and thus is not guaranteed to produce meaningful conclusions because off-gas entrainment is impacted by a host of other variables besides the bubbling flux, such as feed chemistry and melter design characteristics. For example, when the SB6 simulants treated with three different reductants, including formic acid, glycolic acid and sugar, were fed to the DM10 melter, the resulting off-gas from the formic acid-treated feed was found to fluctuate more frequently with greater amplitude than the other feeds.[18] Fluctuating off-gas flow is an indication of off-gas surging, which provides the driving force for the entrainment of non-volatiles.

If the calculated entrainment ratios of the DWPF melter are compared to those of DM1200 at the same bubbling flux of 0.18 scfm/ft^2 solely based on the reductants used, the former are indeed seen to be higher than the latter, except for Fe and Mg, but by a large-than-expected margin. And it does not seem plausible that use of formic acid was the main reason for such a large margin. In fact, focusing only on the major components, the calculated DWPF entrainment ratios of Al, Mn, and U appear to be high, while those of B, Fe, and Si are quite comparable to their respective values of DM1200. On the other hand, the much higher calculated DWPF entrainment ratios of Na and semi-volatiles such as Cd and Cs than their DM1200 counterparts could be reflective of the actual melter conditions leading up to the SB6 pour stream sampling such as extended idling and/or perhaps more frequent and larger-magnitude off-gas surges. In a future study, the calculated entrainment rates of individual species will need to be interpreted by tracking the melter operating history more closely.

Table 7. Comparison of DWPF vs. DM1200 Melter Off-Gas Entrainment Ratios.

Melter	DWPF	DM1200	
Melt Surface Area (ft^2)	28.3	12.9	
# of Bubblers	4[1]	2[2]	
Bubbling Medium	Ar	Air	
Bubbling Rate (scfm)	5.2	2.3	4.7
Bubbling Flux (scfm/ft^2)	0.18	0.18	0.36
Reductant	Formic Acid	Sugar	Sugar
Element	(% Fed)	(% Fed)	(% Fed)
Al	3.3	0.44	0.81
B	1.9	0.90	2.03
Ba	-27.6	0.64	1.38
Ca	-9.5	1.08	1.59
Cd	18.2	2.32	2.68
Cs-137	16.4	-	-
Cu	-628.2	0.60	1.04
F	-	81.58[3]	35.50
Fe	0.7	0.93	1.91
K	46.2	5.21	5.68
Li	0.9	0.44	0.75
Mg	0.2	1.88	3.23
Mn	5.6	0.32	0.66
Na	7.5	1.02	1.88
Ni	-5.6	0.58	1.08
Pb	-36.9	1.10	2.00
Ru	-25.4	4.08	6.18
S	> 49.2	40.39	46.33
Si	0.6	0.35	0.52
Sr	-8.1	1.03	2.29
Th	4.2	-	-
Ti	15.0	-	-
U	4.8	-	-
Zn	-160.4	0.93	1.62
Zr	31.2	0.36	0.64
Overall	2.4	0.62[4]	1.11[4]

[1] Each with one outlet; [2] Each with two outlets; [3] From water dissolution of filter particulate;
[4] Based on gravimetric analysis of filters and rinses
Negative values for DWPF (shown in red text) indicate that the method of matching the ratios to Fe cannot yield meaningful results for these minor components likely because of their high sensitivity to variations in input data.

5.0 Conclusions

The work performed during this study is preliminary in nature since its goal was to demonstrate the feasibility of estimating the off-gas entrainment rates from the DWPF melter based on a simple mass balance using measured MFT batch and glass pour stream composition data and time-averaged melter operating variables over the duration of one canister filling cycle. The only case considered in this study involved the SB6 pour stream sample collected on 12/20/2010 while the melter was agitated with the Ar bubblers. Based on the results presented and subsequent discussions that followed, it is concluded that:

1. The proposed concept of estimating the off-gas entrainment rates from measured feed and pour stream compositions appears feasible at least for the major species and thus additional case studies are warranted. However, success of this approach requires that the analytical data for the feed and pour stream samples carry a high degree of QA pedigree and all required melter operating data be collected, analyzed, interpreted and applied correctly.

2. The overall entrainment rate from the bubbled DWPF melter was calculated to be 2.4% of the calcined solids fed, which is ~2X the design basis entrainment rate for the non-bubbled melter.

3. The average entrainment rate of the four major non-volatile sludge components, including Al, Fe, Mn and U, was calculated to be 2.7% fed, while that of the frit components excluding Na was 0.7%. The higher entrainment rate of sludge over that of frit by a ratio of 4:1 is in qualitative agreement with the analytical results of two deposit samples taken at the inlet of the Quencher.

4. The 4:1 sludge-to-frit entrainment ratio determined in this study for a bubbled melter is ~1/2 that of the non-bubbled melter, which suggests that the frit may become more prone to entrainment when the bubblers are in use.

5. The calculated entrainment rates of Fe, Mg and Si ranged from 0.6 to 0.9% fed, while those of Al, B, Mn, Th and U ranged from 1.9 to 5.6% with Mn at the highest. It is not known why aluminum and manganese showed nearly 5-8X higher entrainment rates than Fe.

6. The calculated entrainment rate of Na was 7.5%, of which a significant fraction could have been entrained via volatilization likely in the form of borates, sulfates, and halides.

7. The calculated entrainment rates of semi-volatile Cs and Cd ranged from 16 to 18% fed, while that of sulfur was estimated to exceed 50%.

8. The calculated DWPF entrainment rates of B, Fe, and Si were comparable to their respective data from the DM1200 melter. For most of the remaining species, the DWPF entrainment rates were higher than the DM1200 results, which may be attributed in part to the use of formic acid as the baseline reductant for the DWPF feeds compared to sugar used for the DM1200 feeds. On the other hand, the much higher calculated DWPF entrainment rates of Na and semi-volatiles could be reflective of actual melter conditions such as extended idling and frequent and/or larger off-gas surges.

6.0 Future Work

The proposed mass balance approach will be tested further against additional pour stream samples taken under different operating conditions (e.g., non-bubbled) and, if necessary, it will be adjusted and refined. In particular, work needs to be focused on resolving the flowrates and melter hold-up of various elements in the process streams in order to obtain a more realistic material balance. Work will also expand to include other isotopes besides Cs-137.

7.0 References

1. EMSP Project Test Plan, "Technetium Management – Hanford Site (FY2015)," ***TP-EMSP-0018***, ***Rev. 0***, U.S. Department of Energy, April 2015.

2. McCabe, D. J., and Choi, A. S., "Task Technical and Quality Assurance Plan for Technetium Management – Flowsheet Modeling Improvements for LAW Recycle Predictions," ***SRNL-RP-2014-01062, Revision 0***, Savannah River National Laboratory, Aiken, SC, October 2014.

3. Matlack, K. S., Weiliang, G., Bardakci, T., D'Angelo, N., Lutze, W., Callow, R. A., Brandys, M., Kot, W. K., and Pegg, I. S., "Integrated DM1200 Melter Testing of Bubbler Configurations Using HLW AZ-101 Simulants," ***VSL-04R4800-4***, ***Rev. 0***, Catholic University of America, Washington D.C., August 16, 2004.

4. Sabatino, D. M., "Sampling Data Summary for the Ninth Run of the Large Slurry Fed-Melter," ***DPST-83-1032***, Savannah River Laboratory, Aiken SC, November 22, 1983.

5. Johnson, F. C., "Analysis of DWPF Sludge Batch 6 (Macrobatch 7) Pour Stream Samples," ***SRNL-STI-2011-00555, Revision 0***, Savannah River National Laboratory, Aiken, SC, February 2012.

6. Choi, A. S., "Validation of DWPF Melter Off-Gas Combustion Model," ***WSRC-TR-2000-00100***, Savannah River National Laboratory, Aiken, SC, June 2000.

7. Zeigler, K. E., and Bibler, N. E., "Characterization of DWPF Melter Off-gas Quencher and Steam Atomized Scrubber Deposit Samples," ***WSRC-STI-2007-00262***, ***Rev. 0***, Savannah River National Laboratory, Aiken, SC, May 2007.

8. Hodges, B. C., *Private Communications*, Savannah River Remediation, Aiken, SC, January- May 2015.

9. Johnson, F. C., "Alternate Reductant Cold Cap Evaluation Furnace (CEF) Phase II Data," ***SRNL-L3100-2014-00081***, Savannah River National Laboratory, Aiken, SC, 2014.

10. Colven, W. P., Sabatino, D. M., Kessler, J. L., and Wolf, H. C., "Summary of the Fifth Run of the Large Slurry Fed-Melter," ***DPST-82-890***, Savannah River Laboratory, Aiken SC, September 29, 1982.

11. Basic Data Report – Defense Waste Processing Facility Sludge Plant, Savannah River Plan 200-S Area, Westinghouse Savannah River Co., Aiken, SC, 1982.

12. Coleman, J. C., *Unpublished Data*, Savannah River Remediation, Aiken, SC, June 2013.

13. Choi, A. S., *PowerPoint Presentation on the 2007 Quencher Deposit Sample Analysis Results*, Savannah River National Laboratory, Aiken, SC, September 2007.

14. Newell, J. D., "Characterization of DWPF Melter Quencher Sample," ***SRNL-STI-2011-00520, Revision 0***, Savannah River National Laboratory, Aiken, SC, November 14, 2011.

15. Johnson, F. C., Stone, M. E., and Miller, D. H., "Alternate Reductant Cold Cap Evaluation Furnace Phase II Testing," ***SRNL-STI-2014-00157***, ***Rev.*** 0, Savannah River National Laboratory, Aiken, SC, September 2014.

16. Jantzen, C. M., "Glass Melter Off-Gas System Pluggages: Cause, Significance, and Remediation (U)," ***WSRC-TR-90-205***, ***Rev. 0***, Westinghouse Savannah River Co., Aiken, SC, March 1991.

17. Johnson, F. C., Choi, A. S., Miller, D. H., and Immel, D. M., "Comparison of HLW Glass Melting Rate Between Frit and Glass Forming Chemicals Using X-Ray Computed Tomography," ***SRNL-STI-2014-00562, Revision 0***, Savannah River National Laboratory, Aiken, SC, April 2015.

18. Choi, A. S., "Melter Off-Gas Flammability Assessment for DWPF Alternate Reductant Flowsheet Options," ***SRNL-STI-2011-00321***, ***Rev. 0***, Savannah River National Laboratory, Aiken, SC, July 2011.

Distribution:

A. P. Fellinger, 773-42A
J. C. Griffin, 773-A
F. M. Pennebaker, 773-42A
T. B. Brown, 773-A
E. N. Hoffman, 999-W
D. H. McGuire, 999-W
S. D. Fink, 773-A
C. C. Herman, 773-A
K. M. L. Taylor-Pashow, 773-A
C. A. Nash, 773-42A
C. L. Crawford, 773-42A
D. J. McCabe, 773-42A
W. R. Wilmarth, 773-A
T. B. Peters, 773-42A
D. T. Herman, 735-11A
A. D. Cozzi, 999-W
K. H. Subramanian, WRPS
Records Administration (EDWS)
J. A. Diediker. DOE-ORP
T. W. Fletcher, DOE-ORP
B. J. Harp, DOE-ORP
C. C. Harrington, DOE-ORP
S. H. Pfaff, DOE-ORP
G. M. Duncan, WTP
S. T. Arm, WRPS
P. A. Empey, WRPS
P. A. Cavanah, WRPS
T. W. Crawford, WRPS
W. G. Ramsey, WRPS
D. J. Swanberg, WRPS
N. P. Machara, DOE-EM
J. A. Poppiti, DOE-EM
D. J. Koutsandreas, DOE-EM
R. A. Gilbert, DOE-ORP
C. J. Winkler, WRPS
R. H. Spires, WRPS
T. W. Crawford, WRPS
S. D. Reaksecker, WRPS
G.K. Allen, WRPS
E. D. Lee, RPP-WTP
R. Gimpel, RPP-WTP